

Design, Fabrication, Modeling and Experimental Study of a Totally Precast Concrete Counterfort Retaining Wall System for Highways

Maen Farhat, Graduate Research Assistant, Dept. of Civil and Materials Engineering,
University of Illinois at Chicago, Chicago, IL 60607, USA

Momenur Rahman, Graduate Research Assistant, Dept. of Civil and Materials
Engineering, University of Illinois at Chicago, Chicago, IL 60607, USA

Mustapha Ibrahim, Graduate Research Assistant, Dept. of Civil and Materials
Engineering, University of Illinois at Chicago, Chicago, IL 60607, USA

Mohsen Issa, Ph.D, F.ACI, F.ASCE, PE, SE, Dept. of Civil and Materials Engineering,
University of Illinois at Chicago, Chicago, IL 60607, USA

ABSTRACT

The overall structural behavior of a Totally Prefabricated Precast Concrete Counterfort Retaining Wall System (TPCCRW) was examined experimentally and analytically using Nonlinear Finite Element Analysis (NLFEA). The 20 ft. high, 13ft-10in. wide full scale TPCCRW prototype was designed meeting the requirements of AASHTO LRFD¹ and manufactured in the precast concrete plant of Utility Concrete Product, LLC in Morris, Illinois. The design was optimized and validated using NLFEA. The wall consisting of face-panel and 3 counterforts were fabricated as a single entity and assembled with the precast base-slab in the field. The key elements were 5 headed anchors extended from each counterfort and grouted in the base-slab through shear pockets to ensure full connectivity between precast components.

TPCCRW was tested experimentally by soil backfilling followed by applying load reaching 192 kips using hydraulic cylinders. The deflection at the face-panel and strain in concrete and steel were instrumented using 7 LVDTs and 45 strain gauges, respectively. The wall experienced a deflection of 0.2 in at its mid-height. The anchors, being the most critical component, succeeded to maintain serviceability and ultimate strength requirements. The furthestmost anchors yielded without affecting the overturning and stability requirements at ultimate load. TPCCRW system has proved to be an innovative solution for multiple requirements such as speed of construction, strength, durability, safety and cost.

Keywords: Accelerated Construction, Assessment and Monitoring, Construction, Creative/Innovative Solutions and Structures, Design-Build

INTRODUCTION

The importance of using precast concrete elements for bridge construction and rehabilitation is considered to be economically efficient as it requires less time of operation².

Although cast-in-place abutments, piers, and deck slabs are being widely used in highway applications, their construction procedures and sequence are considered to be time intensive³. Several activities related to cast-in-place procedures had raised problems on time schedules, safety priorities, and environment. These activities include:

- Site preparation procedures like installation of formwork, casting, curing of concrete
- Traffic detouring and lane closures causing traffic congestion
- Construction works leading to labor exposure to active traffic
- Finishing works that require skilled workmanship.

Precast concrete products are typically made in a controlled plant environment taking advantage of the uniformity and consistency of the high performance concrete properties. Precast concrete bridge components are divided into superstructure and substructure elements. The use of precast concrete technologies in bridge substructure construction has been implemented and frequently reported⁴⁻⁵. The application is mainly focused on precast bent caps, column, and footings.

There have been numerous studies that involved precast concrete bridge components to promote Accelerated Bridge Construction (ABC) in super and sub-structures⁶⁻¹¹. However, scarce literature has been found that covers any development or optimisation for the end supports of bridges like retaining walls and abutments. Precast cantilever retaining wall systems were used in Michigan¹² up to a maximum height of 26 ft. Since the type of wall is regular cantilever wall, a thick wall section was used to control deflection, crack control, and structural design considerations.

An optimization approach of variable heights cast in place counterfort retaining walls was presented taking into account geometric, reinforcement and cost parameters¹³. State of the practice report showed details for connections in precast bridge components including retaining walls and abutments used in different states¹⁴.

An attempt to construct a precast bridge in “only eight days” was made in New Hampshire, 2007¹⁵. The system consisted of precast footing and precast abutment stem. Reinforcement extended from the base footing into predesigned splice sleeves in the stem. These sleeves were grouted by hand using high strength grout through splice ports.

The primary objective is to study the overall structural behavior of a totally prefabricated precast concrete counterfort retaining wall system (TPCCRW). Stability of TPCCRW is maintained through the headed anchors connecting the cantilever part of the wall to the base slab. The anchors play a crucial role in preserving the integrity of the system when subjected to lateral loads.

BACKGROUND

A new and innovative TPCCRW is optimized and developed as a response to the growing needs of multiple requirements such as the speed of construction, strength and durability, minimization interruption of traffic flow, safety and cost.

Striving to construct an efficient precast concrete retaining wall system, the selected design took the form of counterfort retaining wall provided with adequate strength and durability properties. Counterforts act as stiffeners connecting the wall to the base. It has been proven that the counterfort retaining wall system exhibits enhanced serviceability when compared to conventional cantilever retaining wall systems. This is due to the presence of counterforts which act as T-beams along with the face panel of the wall.

As it can be observed in Fig. 1 and Fig. 2, TPCCRW system consists of two prefabricated entities: the wall consisting of a face-panel and three counterforts and the base-slab. Headed anchors are used to connect each counterfort to the base-slab and thus enforcing the integrity of the system as one unit. The precast wall was assembled to the precast base slab in the field where no temporary bracing system was required to accomplish the process.

Five headed anchors were cast and embedded to each counterfort at 1ft. spacing as shown in Fig. 1 to ensure sufficient development length. Starting from the rear face of the face-panel, the first three anchors were #6 and the fourth and fifth anchors were #7. The extended anchors were grouted to the predesigned shear pockets in the base-slab as shown in Fig. 2. The shear pockets in the slab were tapered from 5 in. diameter at the top to 5.5 in. diameter at the bottom to enhance the bond between components. The final TPCCRW assembly is shown in Fig.3.

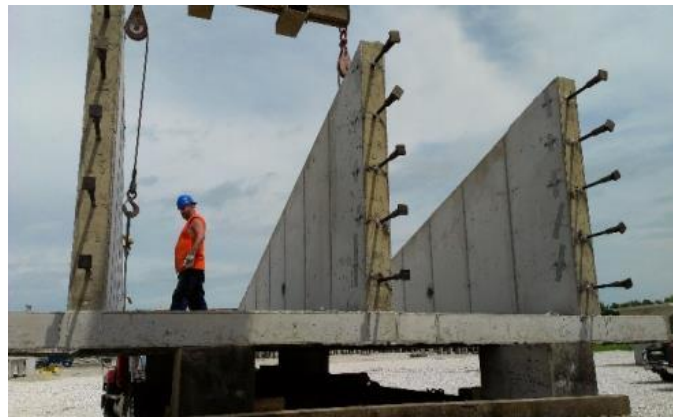


Fig. 1 Anchors extended from the counterfort

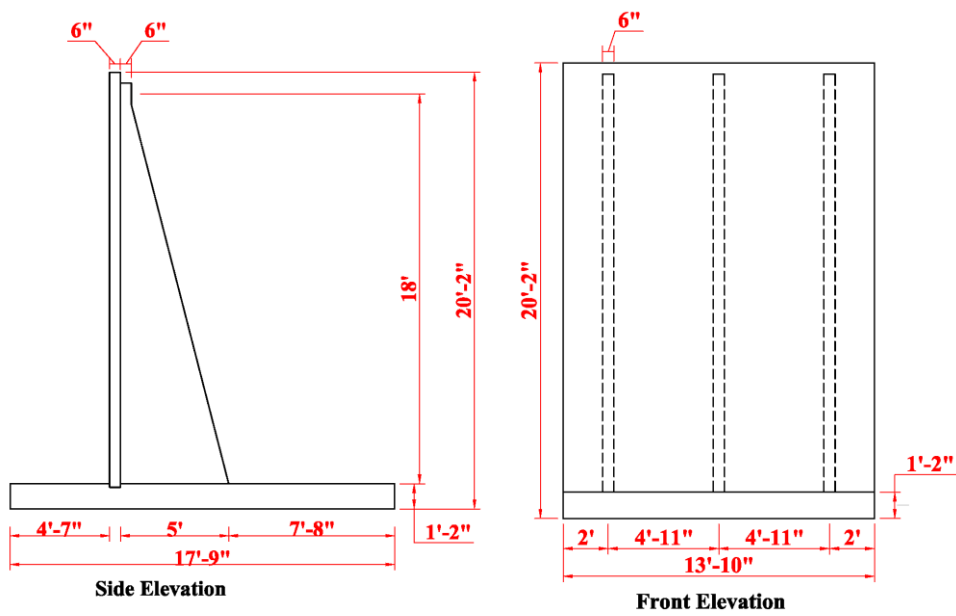


Fig. 2 Predesigned shear pockets in the base slab for anchor embedment



Fig.3 Front elevation TPCCRW with wing walls

The dimensions of the TPCCRW under study are summarized in Fig. 4..



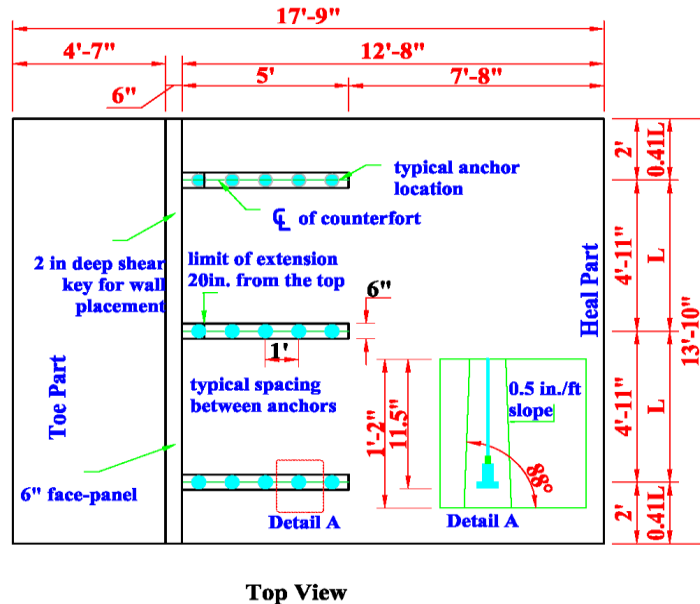


Fig. 4. TPCCRW elevations and dimensions

OPTIMIZATION

Reinforcing the cantilever wall (face-panel) with counterforts will help in reducing the size of the wall considerably while keeping similar level of control over deflections and cracks. The counterforts are with relatively big web extended from the rear face of the face-panel to a certain distance within the heel part of the base slab. As a result, the moments in the face-panel are minimized and a relatively thin concrete face-panel may be used. The number of counterforts within one wall is a matter of critical interest. The use of 3 counterforts was based on the conventional beam theory and the performed finite element analysis (FEA). By conventional beam theory, the bending moment in the face-panel at midspan between counterforts is equivalent to that of the negative moment over each counterfort which is considered to be acting as a support for the face-panel if the length of overhang is made $0.41L$, where L is the spacing center to center between two adjacent counterforts. The resulting distribution of bending and shear stresses allows reduction of face-panel thickness and use of one layer of steel reinforcements. One layer of steel is capable of resisting both positive and negative moments simultaneously, because they are of equal magnitude.

The assembly process is divided into three phases:

1. The placement of the base slab. The base slab has to be leveled and grouted to ensure uniform distribution of the soil pressure generating below the base.
2. Erection of wall which includes the face-panel and the counterforts.
3. Grouting the shear pockets to sustain the required anchorage between the base-slab from one side and the counterforts from the other side through the headed anchors.

This short process allows the erection of retaining walls within a relatively short period compared to the cast-in-place construction.

MAIN PARAMETERS TO BE CONSIDERED IN THE DESIGN OF TPCCRW

1. **Headed Anchor and main steel reinforcements in the counterforts:** Design of the counterfort main steel reinforcements is done by assuming full anchorage to the base-slab. The counterforts are treated as T-beams with the counterfort acting as web and the face-panel as flange. Headed anchors connecting counterforts to base-slab were designed by assuming that they will fully resist the bending moments and shear forces at the bottom of the counterforts
2. **Face-panel:** the design is done by assuming the face-panel a continuous slab spanning over the counterforts and acting as supports.
3. **L-bars connecting the counterforts to the face panel:** L-bars are used to ensure composite action between face-panel and counterforts. They are designed to have sufficient development length inside the counterfort and the face-panel.
4. **Base slab (heel and toe):** The design of the heel in the base-slab is divided into two parts: the cantilever portion extending to the back of the counterforts and the portion between the counterforts as a continuous slab. The heel is subjected to the soil pressure from below and the vertical weight of the soils and surcharge above. The toe part is treated as a cantilever beam subjected to soil pressure from below. It was reinforced by 2 layers of #5 bars at 12 in in both directions.

Fig. 5 summarizes shows the dimensions and detailing of reinforcement in TPCCRW.

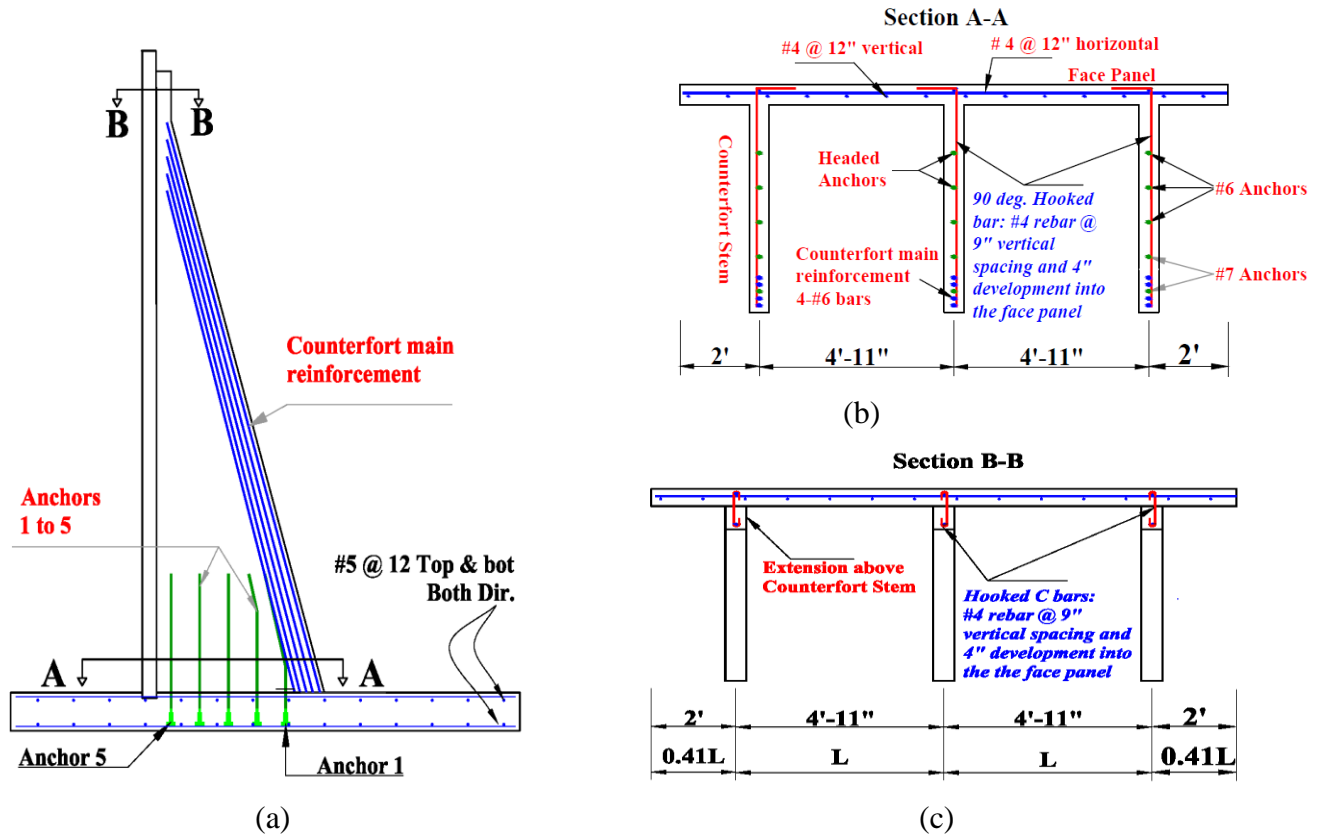


Fig. 5 Side elevation of TPCCRW with section A-A and section B-B

DESIGN LIMIT STATES AND STABILITY REQUIREMENTS

Service I and Strength I design limit states are used for load calculations as per AASHTO LRFD specifications Table 3.4.1-1. The load notations with their load factors are presented in Table 1.

Table 1. Load Notations and Load Factors

Load Description		Notation	Load Factors		
			Service I	Strength I	
				Min.	Max.
Vertical Loads	Self-weight of face panel	DC1			
	Self-weight of base	DC2	1.0	0.9	1.25
	Self-weight of counterfort stem	DC3			
	Vertical earth pressure on the base heel	EV4	1.0		
	Vertical earth pressure on the base toe	EV5		1.0	1.35
	Vertical surcharge load	LS _v	1.0	0.0	1.75
Lateral Load	Horizontal Earth pressure*	P _{EH}	1.0	0.9	1.50
	Horizontal surcharge load	LS _h	1.0	0.0	1.75
	Wind load on structure	P _{ws}	1.0		

*The Horizontal earth pressure is Active

The stability requirements are performed at the Service limit state for the overturning moment, bearing resistance, eccentricity, and sliding. At the strength limit state, stability is checked for bearing resistance, eccentricity and sliding in accordance to AASHTO LRFD 11.6.3.2, 11.6.3.3, and 11.6.3.6 respectively. The system was not studied for overall stability. The total service load calculated using Service I limit state is 152 kip. The total ultimate load calculated using Strength I limit state is calculated to be 253.5 kip. These loads were applied to the finite element model and experimental testing.

MATERIAL PROPERTIES

Material properties utilized in the finite element analysis, design, and experimental testing of TPCCRW and the soil backfill are represented in Table 2. The soil properties were acquired from the geotechnical report. The geotechnical site report indicated the presence of clay soil at the location of testing. For testing purposes, the design considered active earth pressure to assume worst case scenario. However, the results obtained from the experimental testing and the finite element analysis indicated that the deflection at the top of the wall is too small to initiate minimum active pressure as per AASHTO LRFD Table C3.11.1-1. The final design submitted to the precast facility considered at-rest soil conditions.

Table 2. Material properties used in the design and FEA of TCCPRW

Property	Value	Unit	Description
f_y	60	ksi	Reinforcement yield strength
E_s	29000	ksi	Steel modulus of elasticity
f'_c	7100	psi	Concrete strength
γ_c	150	pcf	Unit weight of concrete
E_c	4888	ksi	Modulus of elasticity of concrete
n	6		Modular Ratio, $E_s/E_c = n$, per AASHTO LRFD [5.7.1]
$size_{agg}$	1.0	in.	Maximum aggregate size
γ_s	125	pcf	Dry earth weight
ϕ_s	28.0	deg	Angle of internal friction
k_a	0.361		Coefficient of active earth pressure, AASHTO LRFD 3.11.5.7.1
q_{all}^*	2500	psf	Allowable soil bearing capacity assumed for design
$q_{all_prov}^{**}$	10000	psf	Allowable soil bearing resistance provided by geotechnical
$q_{u_prov}^{**}$	15000	psf	Factored soil bearing resistance provided by geotechnical report

* assumed to obtain work case scenario for weak soil conditions

** actual conditions in the field

The concrete mix design and the results of the concrete average compressive strength properties of each component in the TPCCRW are shown in Table 3. Table 2 shows 7200 psi as the compressive strength value assigned for design and finite element for both the wall and base since it is the lowest value among the tested cylinders.

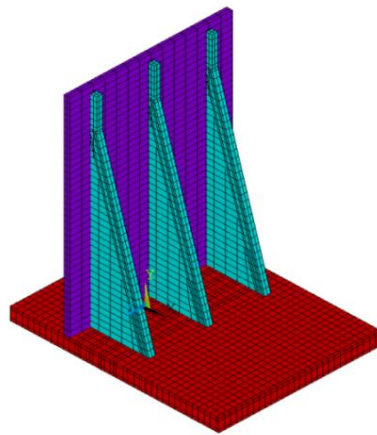
Table 3. Concrete Mix Design for TPCCRW Project.

Material proportions for Mix Design		28 days Concrete compressive strength			
Material	Amount, lbs/yd ³	Specimen	No. of Specimens	Specimen Size	AVG Ult. Stress, psi
Sand	1325	Base	9	6"x12"	9400
Coarse aggregate	1527				
Cementitious materials	700	Wall	7	6"x12"	7280
w/c ratio	0.38				
Air content	6.50%	Grout	4	3"x6"	7660

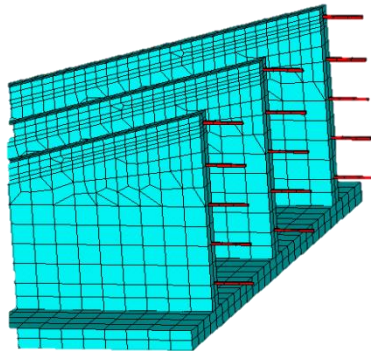
As mentioned earlier, one of the biggest benefits of using precast concrete is to take advantage of utilizing high performance concrete. The excellence of the materials and mixing conditions in the precast yard yield higher compressive strength compared to that used in the cast-in-place industry. This explains the high compressive strength values shown in Table 3.

NONLINEAR FINITE ELEMENT ANALYSIS (NLFEA)

A three dimensional finite element model using ANSYS tools was developed to analyze the structural behavior of TPCCRW as shown in Fig. 6 . The purpose of finite element modeling is to investigate the deflection of wall at top of wall, $H/2$, and $H/3$, where H is the height of wall; evaluate the structural behavior of anchors connecting the counterforts and base-slab; and to verify that the design performed by AASHTO LFRD satisfies structural stability and integrity of the system under both service and ultimate loads.



(a)



(b)

Fig. 6 Finite element model of (a) TPCCRW and (b) anchors extending from counterforts

CONCRETE

SOLID65 element was used to simulate the concrete volume. The element is defined by eight nodes having three degrees of freedom at each node, translations in the nodal x, y, and z directions. It has the capabilities of simulating both cracking and crushing of concrete. The cracking and crushing of concrete is defined by Willam and Warnke model. In this present study, a value of $\beta_t=0.3$ was used for shear transfer coefficient for open crack and $\beta_c=0.9$ for shear transfer coefficient for closed crack. In several studies, the crushing capability of concrete was ignored to avoid fictitious crushing¹⁶⁻¹⁹. Instead a uniaxial multilinear stress-strain concrete cylinder test data of actual test specimen was used to define compressive behavior of concrete. A value of 0.2 was used for concrete's poisson's ratio.

STEEL REINFORCEMENT AND ANCHORS

The steel reinforcement and anchors are modeled using Link8 element. The element is defined as a uniaxial tension-compression element with three degrees of freedom at each node: translations in the nodal x, y, and z directions. The steel material assumed to be bilinear elastic-perfectly plastic that is identical in both tension and compression with elastic modulus (E) of 29,000 ksi and a value of 0.32 was used as poisson's ratio²⁰. The interface between concrete and Link8 elements were assumed to be fully bonded. TARGE 170 and CONTA 174 elements were used to define the frictional interface between the bottom surface of the precast face panel and the top surface of the base-slab.

LOADING AND BOUNDARY CONDITIONS

The retaining wall is assumed to be fully resting on perfectly elastic soil medium. The elastic medium is assigned the elastic foundation stiffness properties. The base slab is assumed to be fully bonded to the elastic medium. Since the purpose of finite element modeling is to investigate the structural behavior of TPCCRW, the simulation of soil-structure interaction under different soil conditions was ignored. The soil reaction underneath the base slab was defined using SURF154 element. SURF154 can be used for various load and surface effect applications²¹. A value of elastic foundation stiffness (EFS) is assigned to represent the equivalent the soil's allowable bearing capacity of 2.5 ksf²³. The analysis was carried out over several load steps. The load steps include self-weight of wall, soil backfilling, and two feet surcharge load in order to simulate the Service I (AASHTO LRFD) load conditions. In addition, a load of 10 kips from the hydraulic cylinders was applied to carry the system to its ultimate load resisting capacity (Strength I) of TPCCRW. The sequence of load steps is (1) self-weight, (2) soil backfilling, (3) two feet of surcharge live load, and (4) 200 kip load applied at H/3 to reach the ultimate strength resistance (Strength I) of the wall.

The loads were calculated per AASHTO LRFD and applied in the finite element model as nodal loads. Horizontal component of soil backfills (linearly increasing from top to bottom of wall) and surcharges load (constant along height of wall) were distributed on all nodes at the inner face of wall. The vertical component of soil backfills and surface load were evenly distributed on top surface of base slab. The 200 kip load was applied at one third height of wall ($H/3$).

DISCUSSION AND ANALYSIS OF NLFEA RESULTS

The deflections of the wall as well as the variation of the strain in the concrete, steel reinforcement, and anchors are discussed below.

Load vs. Deflection curve

The loads assigned to the model are self-weight of the TPCCRW, lateral pressure due to soil backfilling and a load of 200 kips applied by the hydraulic cylinders at $H/3$ of the wall at each counterfort. The applied load vs deflection curves and the deflections contours of TPCCRW at different heights of face panel are shown in Fig. 7 and Fig. 8, respectively. Inspection of Fig. 7 reveals that, under service loads, the deflection at top of wall is estimated to be around 0.13 in (3.30 mm). In addition, the deflections at mid-height ($H/2$) and one third height ($H/3$) of the wall were calculated to be 0.072 in (1.78 mm). and 0.042 in. (1.07 mm), respectively. At ultimate load (253.5 kips) the top of wall deflects 0.21 in (5.33 mm). And the deflections at mid-height ($H/2$) and one third height ($H/3$) of wall are 0.12 in (3.05 mm) and 0.09 in (2.28 mm) respectively.

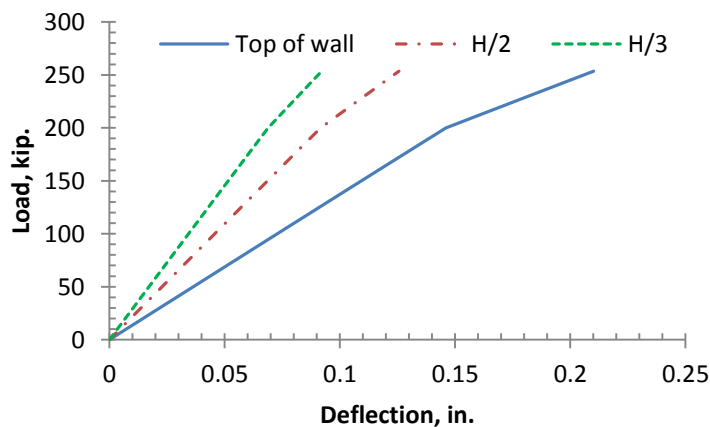


Fig. 7 Load vs. deflection plots using ANSYS Package

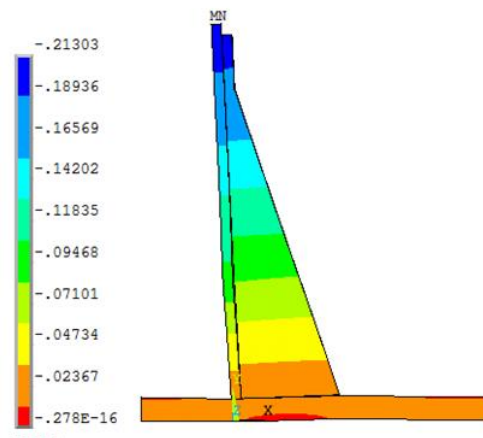
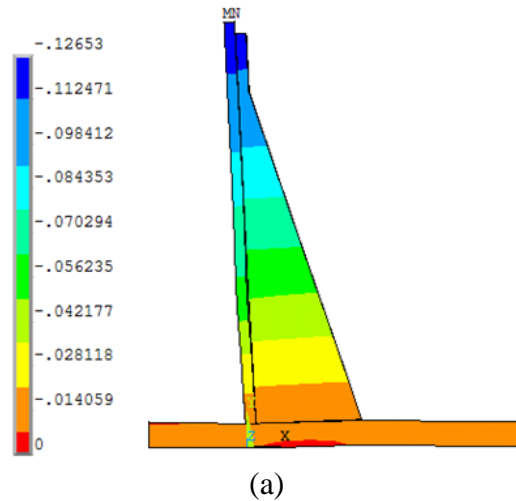


Fig. 8 Deflection contour at (a) service load (152 kip) (b) ultimate load (253.5kip) (ANSYS Package)

Stress vs. strain results in anchors

The behavior of the anchors in the middle counterfort was examined as it is subjected to more loads than the exterior counterforts. The strain variation in the anchors for the middle counterfort are presented in Fig. 9 . Inspection of Fig. 9 reveals that, upon examining the curves, the strain results values indicate a decreasing general trend starting from the outermost anchor approaching the face of the face-panel as expected. The anchor analysis reveals that anchor1, the furthest anchor from the face-panel (#7 anchor), has yielded at a load of 175 kips. Anchor 2 shows yielding strain of $2069 \mu\epsilon$ at 253.5kips . However, it can be observed that anchor 3 is close to yielding since the actual loading conditions can be higher.

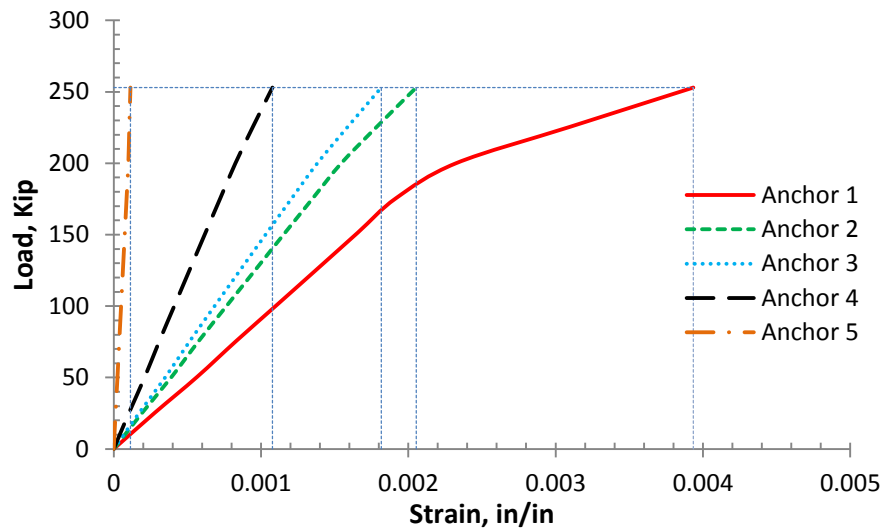


Fig. 9 Applied load vs. strain at each anchor in the middle counterfort from ANSYS

EXPERIMENTAL PROGRAM

FABRICATION

TPCCRW is formed of two totally precast components; the face-panel and counterforts cast as one component and the base-slab as separate component. Based on the analysis and calculations, the face-panel and counterforts were reinforced with one layer of steel reinforcement. Fig. 10 shows the L-bars extended from the face-panel to the counterfort. The base-slab was reinforced with two identical layers. The steel reinforcement of the TPCCRW at the level of each component is summarized in Table 4.

Table 4. Reinforcement Details at All Wall Sections

Assembly Part	Number of layers	Vertical	Horizontal	Inclined
Face	1	#4 @ 12	#4 @ 12	--
Counterfort	1	#4 @ 12	#4 @ 6	4 # 6
Base	2	#5 @ 12	#5 @ 12	--
Anchors	--	2#7 and 3#6 on each counterfort		

Each counterfort is connected to the base-slab using 5 headed anchors. Each headed anchor is embedded 11.5 in. in the base-slab. The anchors are at 1 ft. spacing starting at 6 in. from the internal face of the wall. The development length of the L-bars can also be reduced by reducing the spacing between them.



Fig. 10 Fabrication process of wall face and counterforts showing extended L-bars

INSTRUMENTATION

The purpose of instrumentation is to monitor the structural behavior of the retaining wall during all loading stages. The loading stages start with soil backfilling and end with applying loads using hydraulic cylinders.

LVDTs were placed against the face-panel of the wall at seven different locations. Four of them are at one third of the height of the wall and three at mid-height of the wall. The purpose of this configuration is to study the deflection of the wall at the counterforts and at the mid-span between them. The seven LVDTs were fixed to a steel frame against the wall and connected to a portable data logger system that would provide instantaneous reading of the wall deflection.

Forty two strain gauges were installed at different locations. Twelve strain gauges were mounted on concrete and the rest were mounted on steel covering the critical locations of the TPCCRW such as the anchors, the face-panel, the base-slab, and the main reinforcement in the counterforts and extensions above the counterfort. A typical LVDT and strain gauge attachment to the face-panel is shown in Fig. 11.

For the face-panel, strain gauges were used to study the response of the steel at the locations of positive (mid-span) and negative moments (at counterfort).



Fig. 11 Strain gauge and LVDT on concrete surface

ERECTION

The erection process starts at the level of the base-slab. The base-slab was cast, then delivered to site after curing. It was placed 2ft. below grade level on spacers which guaranteed a 1 in. offset from the ground in order to allow for grouting below the base. The base was grouted to eliminate any voids so that the base would rest uniformly on the ground. The grout was pumped through four holes until all the voids below the base were filled. Fig. 12 shows the erection of the base-slab with the grout holes and Fig. 13 shows the final assembly of TPCCRW. After placing the base-slab, the wall was erected through placing the headed anchors in the shear pockets of the base slab and filling them with high strength and fast setting (15 minutes) grout.

Two circular holes were designed and made in each of the two external counterforts for handling purposes. Steel cylinders were inserted in each hole and the wall was carried by steel cables wrapped around the steel cylinders. The effect of wind load on the stability of the system during construction was calculated and was found to be negligible. As a result, the crane was capable of handling the wall without a need for a temporary bracing system.



Fig. 12 Finishing the erection of the base slab



Fig. 13 Final assembly of TPCCRW

SETUP AND TESTING PROCEDURE

The retaining wall was tested and monitored against soil pressure and surcharge load in the following order:

1. Soil Backfilling: soil pressure was applied by filling the back of the retaining wall with soils where 95% compaction level was maintained.
2. Surcharge Load: was applied using Dozers to simulate the actual condition for live surcharge.
3. Test 1: two hydraulic cylinders applied up to 178 kips at one H/3 of the wall acting at 6 points divided over 3 counterforts. It is followed by Hydraulic actuator at the top of the wall delivering 160 kips.
4. Test 2: two hydraulic cylinders applied up to 136 kips at H/3 of the wall acting at 6 points divided over 3 counterforts.
5. Test 3: two hydraulic cylinders applied up to 97 kips at H/3 of the wall acting at 2 points on middle counterfort.
6. Test 4: two hydraulic cylinders applied up to 192.4 kips at H/3 of the wall acting at 6 points divided over counterfort.

Soil Backfilling

The first step in performing the experimental testing is the soil backfilling. Soil Pressure was applied on the wall by backfilling soil behind the wall. The soil was filled at 6 in. increments. At each increment soil is compacted using a sheep-foot roller compacting machine. The goal was to maintain 95% compaction level. The proctor test revealed that the wet density of the soil is 130pcf. The moisture level by the end of backfilling was estimated to be 12 %. The top surface of the soil was finished at almost a leveled surface.

Surcharge load

In order to imitate the surcharge load stated by AAHSTO LRFD that would account for the live load. Two vehicular live loads were placed at the top of the backfill. The first vehicle is a smaller bulldozer weighing 27 kips. Afterwards, it was replaced by a bigger bulldozer weighing 37 kips. The bulldozer was placed 2 ft. away from the wall to maintain a worst case scenario as shown in Fig. 14. The live load application was also followed by placing a hydraulic cylinder which was used to apply a lateral load of 16 kips at the top of the wall mounted against the bulldozer.



Fig. 14 application of live load surcharge using a 37 kip bulldozer

Applied Load Testing using hydraulic cylinders: Test 1-4

Tests 1 to 4 were performed using two hydraulic cylinders of 150 ton ultimate capacity each. The test setup is shown in Fig. 15. The cylinders were anchored to a pile of ten concrete blocks each weighing around 18 kips to 25 kips. Four steel cables, 1.5 in. diameter each, were hooked to the hydraulic cylinders from one side and to a 7 in diameter steel solid rod. The steel rod held six steel cables of 3/4 in. in diameter. The six steel cables in turn were connected to the wall through 3 in. diameter holes made especially for this test. The wall was loaded by placing three steel rods of 3 in. diameter each in special openings made in the counterfort at $H/3$.



(a)



(b)

Fig. 15 Experimental test setup showing hydraulic cylinders and steel rod

ANALYSIS OF TEST RESULTS

The test is supported by a finite element analysis to study the behavior of the wall subjected to backfill and additional loading.

DEFLECTION RESULTS

A sample of the deflection results is represented in Fig. 16 and Fig. 17. The two figures show the deflection variation over the whole testing period. The data was collected continuously

throughout the scope of the project. The times of the testing are marked in the figures. After each test was executed, the load was removed. The 3 LVDTs located at H/2 showed very similar readings. The deflections at H/2 showed a maximum value of 2.5 mm (0.1 in.) at the end of backfilling, 2.9 mm (0.115 in.) by adding the surcharge loading, and 4.01 mm (0.158 in.), 4.01 mm (0.158 in.), 4.16 mm (0.163 in.), and 5.4 mm (0.212 in.) at Tests 1, 2, 3 and 4, respectively.

Deflection results show that the critical locations at left midspan, middle counterfort and right midspan at H/3 of the wall exhibit a very similar behavior. The deflection of the fourth location at the left counterfort is slightly higher. Inspection of Fig. 17 shows that the maximum deflection at H/3 is recorded during Test 4 and found to be 4.25 mm (0.167 in.) at the left counterfort. A slightly smaller value of 3.55mm (0.14 in.) was recorded by the 3 other LVDTs at the same level.

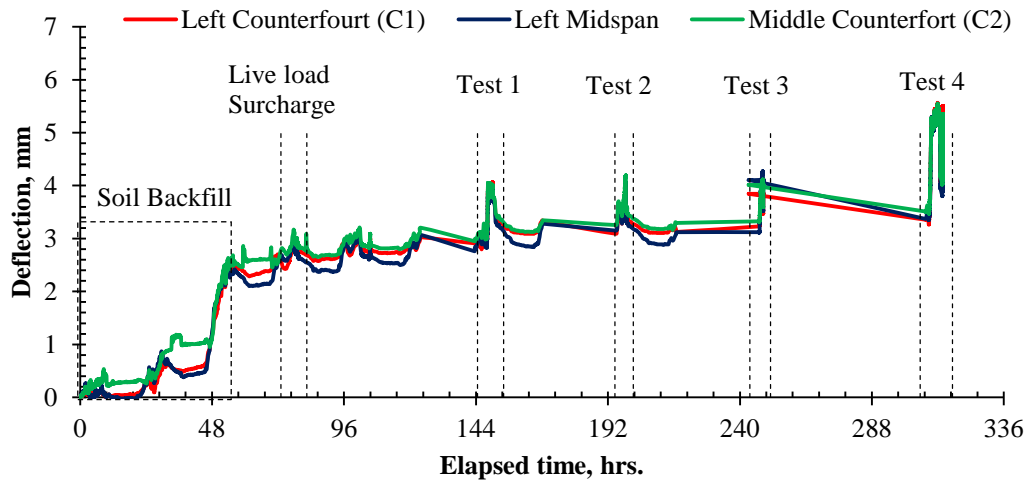


Fig. 16 Deflection measured by the 3 LVDTs at H/2

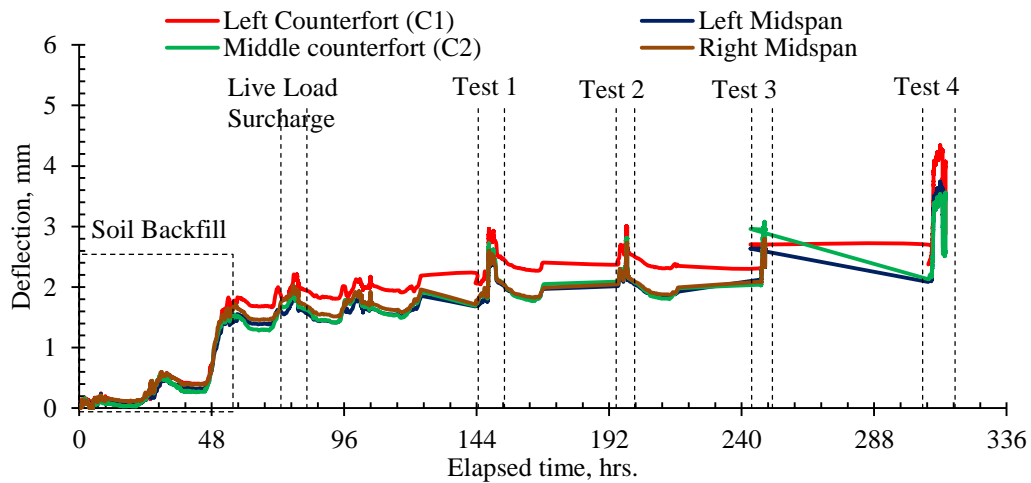


Fig. 17 Deflection measured by the 3 LVDTs at H/3

STRAIN IN THE ANCHORS

The maximum strain readings in the headed anchors at the middle and left counterforts are presented in Fig. 18 **Error! Reference source not found.** Inspection of Fig. 18 reveals that the strain results at the headed anchors showed quite some variation depending on the location of the anchor with respect to the wall and location of the counterfort. The outermost two anchors from the wall experienced the highest strain readings due to their longer moment arm with respect to the wall. These readings gradually decrease in the anchors closer to the wall in almost linear fashion. The strain readings in anchors 1 and 2 at the middle counterforts were found to be 2659 $\mu\epsilon$ and 2203 $\mu\epsilon$. Therefore, anchors 1 and 2 of the middle counterfort exceeded the 2070 $\mu\epsilon$ which is the yield limit of steel. The strain readings in anchors 1 at the left counterfort was found to be 2421 $\mu\epsilon$ and thus exceeding the 2070 $\mu\epsilon$. however the reading of anchor 2 showed that it is on verge of yielding with 2010 $\mu\epsilon$.

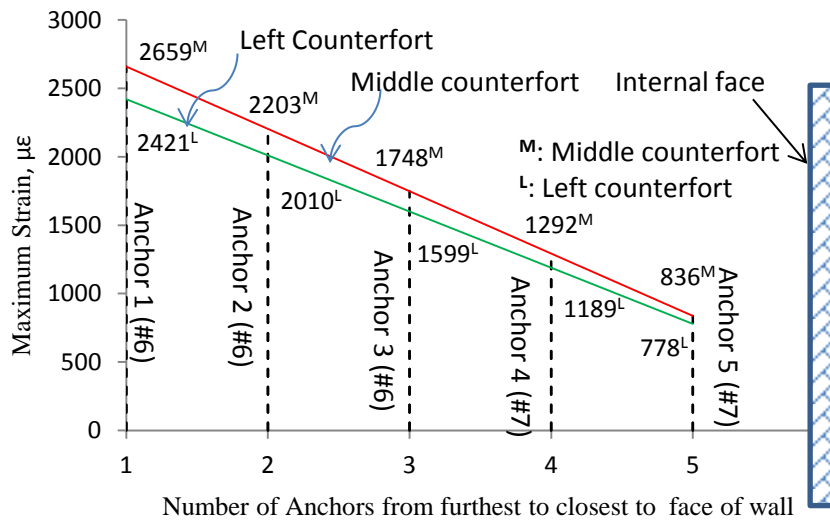


Fig. 18 Maximum strains in headed anchors at the middle and Left counterforts

The strain variation at the testing times for Anchor 1 (#7) located at the left counterfort throughout various loading conditions is shown in Fig. 19. During soil backfilling, the strain increased up to 1360 micro-strains ($\mu\epsilon$). It was then followed by gradual increase throughout the scope of testing. This increase takes the form of sharp spikes at the time of testing where the load was applied by hydraulic cylinders. The spikes were followed by sharp drops as soon as the load was removed. This is due to the fact that anchor steel did not yield until the test was loaded to an ultimate load at Test 4. The yielding limit of the anchor was observed in Test 4 where it reached 2421 $\mu\epsilon$ when subjected to 192400 lbs. ultimate load. The curve also shows a repetitive trend of gradual increase and decrease in the strain readings over time. The gradual drop in the strain reading was observed to occur during

nighttime and vice-versa during the day. This might be attributed to the temperature variation between day and night as the test was performed in field conditions.

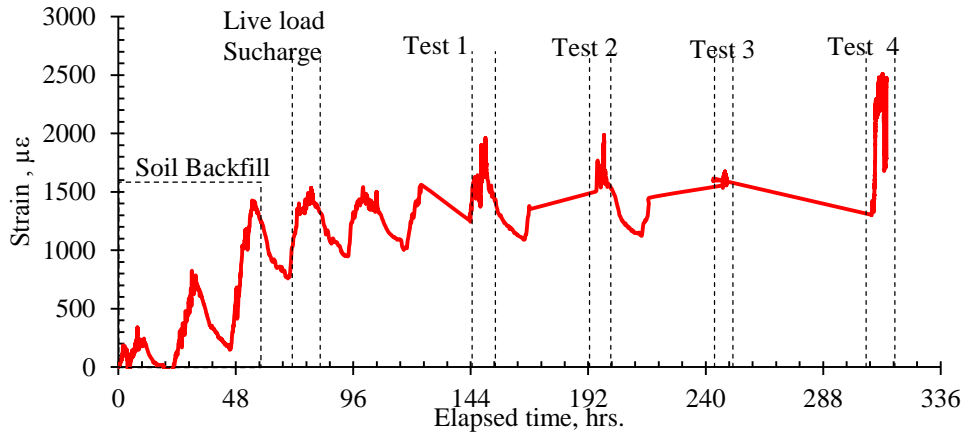


Fig. 19 Strain variation curve at the times of testing for Anchor 1 in Left Counterfort

FACE-PANEL AND COUNTERFORT MAIN REINFORCEMENT

No visible cracks were initiated at the front face of the face-panel. This is attributed to the efficiency of the geometric configuration that helped lowering the stresses in the face-panel and achieved a successful design using one layer of steel with 6 in. wall thickness. The results showed that no yielding occurred in the main reinforcement of the face-panel. Fig. 20 represents sample strain readings at the left midspan between counterforts and over the middle counterfort. The maximum strain readings at H/3 at the midspan between the counterforts and over the counterforts were similar and ranged from 500 to 600 µε as shown in Fig. 20.

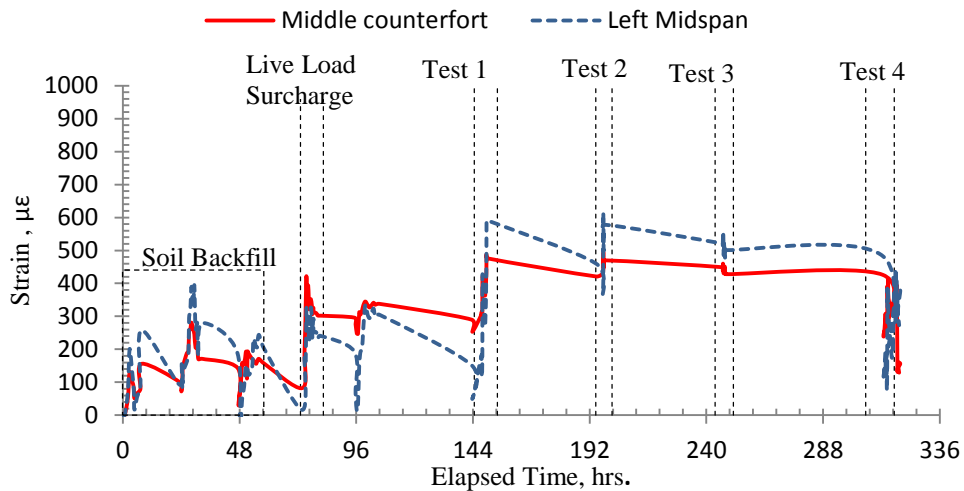


Fig. 20 Strain vs. time readings for face-panel steel reinforcement located at H/3 at the middle counterfort and left midspan

On the other side after investigating the strain results at the counterforts main reinforcement, It is possible that yielding did not occur in the inclined main reinforcement of the middle and right counterforts with maximum strain reading not exceeding $1000 \mu\epsilon$. However, it is more likely that cracks developed in the concrete at the level of inclined surface to counterforts, 3 ft. from the bottom, due to high overturning moment resisted by the T-section of the counterforts and the face-panel. This was validated using finite element analysis as shown in

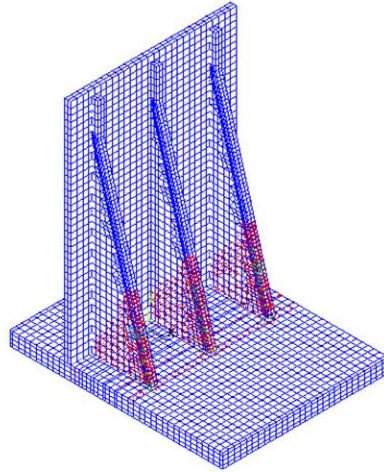


Fig. 21. Development of cracks in the counterforts and base slab at ultimate load.

STRAIN IN THE BASE SLAB

The analysis of the strain reading of steel reinforcement at the top layer of the base slab shows that the strain reading is influenced by the type of loading. At the time of backfilling it is noticed that strain readings exhibited a fluctuating behavior. This is due to the vertical load applied during backfilling by the soil weight and the live load of the excavation vehicles. Once the lateral load is applied a drop in the strain reading is noticed indicating the increase of tensile stresses at the top layer as shown in Fig. 22.

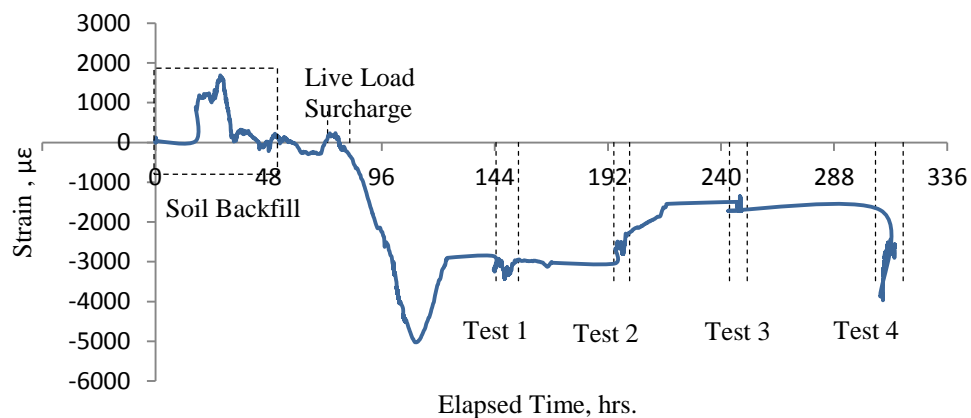


Fig. 22. Strain vs. elapsed time in steel at top reinforcement of the base 1 ft. from middle counterfort

COMPARISON BETWEEN NLFEA AND EXPERIMENTAL RESULTS

The calculated deflection from NLFEA results at mid height of wall ($H/2$) and one third of wall at service load were 1.78 mm (0.072 in) and 1.07 mm (0.042in) respectively. From experimental results, the maximum deflection measured at mid height of wall ($H/2$) and one third of wall ($H/3$) from 3 LVDTs were 2.9 mm (0.115 in.), and 2.01 mm (0.079 in), respectively. The experimental results showed higher deflection than NLFEA results was expected due to the fact the finite element model assumed the base slab to be bonded to the elastic foundation. This means that the base slab is restricted from sliding in the lateral direction. However, in the experimental results, very slight sliding might have occurred. The deflection readings include the absolute deflection in the wall plus the sliding value.

The results obtained at the headed anchors using the finite element analysis shows a good correlation with the experimental results. The finite element analysis shows that at ultimate load, the strain is estimated to be around $2320 \mu\epsilon$ in the outermost anchor at 192.4 kips load (Test 4). Also, the trend obtained from the finite element analysis at ultimate load shows that yielding occurs at the first two anchors (Anchors 1 and 2). The strain readings in the anchors decrease as we go closer to the face-panel (moving from anchor 1 to 5).

CONCLUSIONS

Based on the experimental test and the FEA results, the following can be concluded:

1. A counterfort-spacing to height ratio equals to 0.245 proved to be an optimum design in resisting the applied service and ultimate loads.
2. Stability of the wall was maintained at service and ultimate loads. Stability include stability against overturning, sliding, eccentricity, and bearing capacity.
3. TPCCRW showed good performance in resisting the applied loads. The stability and strength requirements were satisfied.
4. The main reinforcement in the counterforts showed a good performance as expected based on the strain readings at service and ultimate loads.
5. The anchors are the key elements in maintaining the system stability. It showed excellent performance in maintaining the composite action between the precast wall and the base slab at service and ultimate loads. This was verified by the NLFEA and the experimental testing.
6. The deflection measured at the mid-height of the wall was found to be around 0.2 in. Counterforts added stiffness to the structure by increasing the section at which the bending moment due to the applied load is being resisted. The L-bars that connected the face-panel to the stems was found to be very effective in maintaining the composite action between both components.
7. TPCCRW can be utilized for highway applications. It satisfies the need for fast track construction. Although the impact factor specified by AASHTO LRFD specifications was implemented in the design, further research might be required to study the behavior of TCCRW under traffic collision force.

ACKNOWLEDGEMENT

The study was funded and supported by Utility Concrete Products (UCP), LLC. Morris, IL. Thanks for UCP for performing the fabrication, erection, and providing all the means for the experimental testing that was performed at the UCP facility. In addition, Thanks to Claudio Fazio from V3 for providing the preliminary design criteria. Special thanks for all who provided help and support to achieve this work.

REFERENCES

1. American Association of State Highway and Transportation Officials, 2012, AASHTO LRFD bridge design specifications: customary U.S. unit,
2. Biswas, M., 1986, "Precast Bridge Deck Design Systems," *PCI Journal*, V. 31, No.2, Mar.-Apr., pp. 40-94.
3. Hieber D., Wacker J., Eberhard M., Stanton J., "State-of-the-art report on precast concrete systems for rapid construction of bridges", . WA-RD 594.1.
4. Medlock, R., Hyzak, M., and Wolf, L., "Innovative Prefabrication in Texas Bridges," *Proceedings of the Texas Section, ASCE, Spring Meeting, 2002*, pp. 1-6.
5. Joshua T. Hewe,"Analysis of the State of the Art of Precast Concrete Bridge Substructure Systems", *AZTrans: The Arizona Laboratory for Applied Transportation Research*, Final Report FHWA-AZ-13-687,2013,PP.124
6. Billington, S.L., Barnes, R.W., and Breen, J.E., "Alternate Substructure Systems for Standard Highway Bridges," *Journal of Bridge Engineering*, V. 6, No. 2, Mar.-Apr.2001, pp. 87-94.
7. Billington, S., Barnes, R., and Breen J., "A Precast Substructure Design for Standard Bridge Systems", *Project Summary Report 1410-2F, Center for Transportation Research, University of Texas at Austin*, 1999, 170 pp.
8. Culmo, M.P., "Bridge deck rehabilitation using precast concrete slabs," *Eight Annual International Bridge Conference*, Paper No. IBC-91-55,1991, pp. 389-396.
9. Culmo, M.P., "Rapid bridge deck replacement with full-depth precast concrete slabs," *Transportation Research Record 1712*, Transportation Research Board, Washington D.C., 2002, pp. 139-146.
10. Badie, S.S., Baishya, M.C., and Tadros, M.K., "NUDECK- An efficient and economical precast prestressed bridge deck system," *PCI Journal*, V. 43, No. 5, Sept.-Oct.,1998, pp. 56-74.
11. LoBuono, Armstrong, and Associates, "Development of Precast Bridge Structures," *Report Prepared for Florida Department of Transportation*,1996, pp. 1-25.
12. Darwish,I., and Kasi, M., Alfred Benesch& Company. "Innovative Precast Concrete Cantilever Retaining Wall System". *ASPIRE*, Spring 2013 page 2. (2013)
13. Donkada, S., and Menon, D., (2012). "Optimal design of reinforced concrete retaining avails". *The Indian Concrete Jornal*. April 2012, pp. 9-18.
14. Culmo, M.P.,March, "Connection Details for Prefabricated Bridge Elements and Systems," FHWA-IF-09-010, 2009, pp. 568.

15. Stamnas, P. E.,Whittemore, M. D., New Hampshire Department of Transportation, “Precast Bridge Built in only Eight Days”, *ASPIRE*, Spring 2007, PP. 22-25
16. Kachlakev, D., Miller, T., Yim, S., “Finite element modeling of reinforced concrete structures strengthened with FRP laminates”, Oregon Department of Transportation, Salem, Oregon, May 2001.
17. ANSYS User’s Manual (Release 11.0 Documentation), ANSYS, Inc., Canonsburg, Pennsylvania, USA
18. Zhou S, Rizos D C and Petrou M F , “Effects of Superstructure Flexibility on Strength of Reinforced Concrete Bridge Decks,” *Computers & Structures*, 82(1), 2004, pp. 13-23.
19. Si, B.J., Sun, Z.G., Ai, Q.H., Wang, D.S., and Wang, Q.X., “Experiments and simulation of flexural-shear dominated RC bridge piers under reversed cyclic loading”.*The 14th World Conference on Earthquake Engineering*, October 12-17, 2008, Beijing, China
20. Al-Rousan, R., Issa, M., “Fatigue performance of reinforced concrete beams strengthened with CFRP sheets”, *Construction and Building Materials*, Volume 25, Issue 8, August 2011, pp. 3520-3529.
21. Bowles, E. J., “Foundation analysis and design”. *McGraw-Hill*. ISBN-0-07-912247-7, 1996, pp. 313-317.